Interaction of mucin with viologen and acetate derivatives of calix[4]resorcinols

Summary of the article:
5280 words (excluding 44 references, abstract and keywords)
6 figures
1 table

Interaction of mucin with viologen and acetate derivatives of calix[4]resorcinols

Ruslan R. Kashapov*[a,b], Nadezda E. Kashapova[a], Albina Y. Ziganshina[a], Victor V. Syakaev[a], Vitaliy V. Khutoryanskiy[c], and Lucia Y. Zakharova[a,b]

[a]Arbuzov Institute of Organic and Physical Chemistry, FRC Kazan Scientific Center of RAS, 8 Arbuzov Str., 420088 Kazan, Russia

[b]Kazan National Research Technological University, 68 Karl Marx Str., 420015 Kazan, Russia

[c]School of Pharmacy, University of Reading, Whiteknights, Reading, RG66DX, United Kingdom

[*]Corresponding author at: Arbuzov Institute of Organic and Physical Chemistry, FRC Kazan Scientific Center of RAS, 8 Arbuzov Str., 420088 Kazan, Russia. E-mail address: kashapov@iopc.ru (R.R. Kashapov). Phone number: +7 (843) 273-22-93

Abstract

The mucus layer acts as a selective diffusion barrier that has an important effect on the efficiency of drug delivery systems in the human body. In this regard, currently the drug nanocarriers of various sizes and compositions are being widely developed to study their mucoadhesive properties i.e., the ability to interact with mucin. However, the effective interaction of drug composition with mucin does not guarantee the success due to the fact that there is a further barrier in the form of epithelial cells retained by calcium ions under the mucus layer. In this work, the interaction of mucin (porcine gastric mucin) with calixarenes is considered for the first time. The study of interaction between calixarenes, mucin and calcium ions by a complex of physicochemical methods showed that effective interaction with mucin requires cationic fragments, and binding with calcium is realized due to anionic fragments in the calixarene structure. Therefore, the combination of different chemical groups in the structure of drug nanocarrier plays an important role in successful mucosal drug delivery. Taking into account the

wide possibilities of synthetic modification of the macrocyclic platform, calixarenes can find the application in the drug delivery across mucous barriers.

Key words: mucin, mucoadhesion, self-assembly

1. Introduction

The properties of mucosal surfaces are governed by the presence of mucin glycoproteins, which are secreted by specific epithelial cells. The epithelial cells are held together with the help of tight junctions, which contain calcium ions.[6] Hence, the development of drug nanocontainers capable of interacting with mucins and calcium ions is of special interest. Moreover, recently the ability of the severe acute respiratory syndrome coronavirus to bind to mucosal epithelial cells was discovered, which forms the main target site of corona-virus infections.[7] This indicates that disruption of the mucus barrier for improved drug delivery to underlying cells is an important property of drug nanocarriers to penetrate the mucosal epithelial cells.

Supramolecular compositions involving macrocyclic molecules are of particular interest not only due to their ability for molecular recognition, but also as precursors for developing novel nanomaterials for pharmaceutical and biomedical applications. Since the important directions in the development of nanomedicine are targeted drug delivery using nanoparticles and controlled release of drug from nanoparticles to target without damaging the surrounding tissues, it can be assumed that the use of macrocycles, which can be modified by certain chemical groups, is highly promising for these purposes. Among different macrocyclic compounds, calixarenes are identified as the widely investigated molecular scaffolds in supramolecular chemistry.[8] The most commonly studied calix[4]arenes have four phenolic units linked in the cyclic structure by methylene groups.[9,10] These phenolic moieties can freely rotate along the methylene bridge, and calix[4]arenes can adopt several interconvertible conformations. The advantages of calixarenes include their synthetic versatility, and also rigid architecture.[11] Calix[4]resorcinols, the products of condensation of resorcinol and aldehyde, represent an example of macrocycles with a rigid structure. The substitution of upper and lower rims of calix[4]resorcinol restrict the conformations of the macrocycle. Similar to calix[4]resorcinols, calix[4]resorcinol cavitands have a molecular cavity formed by four aromatic resorcinol moieties, but they are more conformationally rigid due to the bridging of oxygen atoms of the adjacent aromatic rings.[12]

For the modification of mucoadhesive systems, cyclodextrins are sometimes used as drug delivery systems.[13] Encapsulation of hydrophobic drugs in the cavity of cyclodextrins allows preparing water-soluble dosage forms, which favorably affects the therapeutic effect. There are also some studies demonstrating the potential porphyrins[14] and crown ethers[6] for transmucosal

drug delivery. While porphyrin molecules only provided the cancer targeting, polyether molecules not only increased the water solubility of the drug, but also extracted calcium ions from the corneal epithelium, which weakened the tight junctions of epithelial cells, enhancing drug penetration into the cornea *in vitro*.

Considering the possibilities of modifying the rims of the calixarene platform with various functional groups, these macrocycles offer an excellent class of materials to develop novel mucoadhesive drug delivery systems. It is surprising that so far no one has studied the interaction of mucin with calixarene derivatives. In the present paper, we investigated the amphiphilic calix[4]resorcinols bearing viologen groups (**VC5**, **VC10**) and calix[4]resorcinol bearing acetate groups (**AC10**) at the upper rims (Figure 1) for their ability to interact with mucin, to bind caffeine (a water-soluble model drug), and to form complexes with calcium ions.

2. Materials and methods

2.1. Chemicals and reagents

Calix[4]resorcinols **VC5**, **VC10**, and **AC10** were synthesized according to previously reported procedures[15,16]. Mucin, from porcine stomach (Type III, bound sialic acid 0.5-1.5%, partially purified powder, Sigma-Aldrich), caffeine (Sigma-Aldrich), calcium chloride of chemically pure grade, phosphate buffered saline, PBS (tablet, pH 7.4 at 25^0C, Sigma-Aldrich), and D_2O (99.9 atom% D, Carl Roth GmbH) were used as received. Sample solutions were prepared in deionized water (18.2 MΩ) obtained from a Millipore Direct-Q 5 UV water purification system.

2.2. Methods

2.2.1 NMR spectroscopy

All NMR experiments were performed on a Bruker AVANCE(III)-500 spectrometer. The spectrometer was equipped with a Bruker multinuclear z-gradient inverse probe head capable of producing gradients with strength of 50 G cm^{-1}. All experiments were carried out at 303±0.2 K. Chemical shifts were reported relative to HDO (4.7 ppm) as an internal standard.

The Fourier transform pulsed-gradient spin-echo (FT-PGSE) experiments[17–19] were performed by BPP-STE-LED (bipolar pulse pair–stimulated echo–longitudinal eddy current delay) sequence[20]. Data were acquired with a 50.0 and 75.0 ms diffusion delay, with bipolar gradient pulse duration from 1.4 to 4.2 ms (depending on the system under investigation), 1.1 ms spoil gradient pulse (30%) and a 5.0 ms eddy current delay. The bipolar pulse gradient strength was varied incrementally from 0.01 to 0.32 T/m in 16 steps. The temperature was set and controlled at 303K with a 640 l/h airflow rate in order to avoid any temperature fluctuations owing to sample heating during the magnetic field pulse gradients.

The diffusion experiments were performed at least three times and only the data with the correlation coefficients of a natural logarithm of the normalized signal attenuation ($\ln I/I_0$) as a function of the gradient amplitude $b = \gamma^2\delta^2g^2(\Delta-\delta/3)$ (γ is the gyromagnetic ratio, g is the pulsed gradient strength, Δ is the time separation between the pulsed-gradients, δ is the duration of the pulse) higher than 0.999 were included. Experimental data were processed with the Bruker TopSpin software package (version 3.2). The diffusion constants were calculated by exponential fitting of the data belonging to individual columns of the pseudo 2D matrix. Single components have been assumed for the fitting routine. All separated peaks were analyzed and the average values were taken.

The pulse programs for all NMR experiments were taken from the Bruker software library.

2.2.2. Fluorescence spectroscopy

Fluorescence measurements were recorded using a Hitachi F-7100 Fluorescence Spectrophotometer equipped with a xenon lamp source, a 10 mm path length quartz cell and a thermostat bath. Steady state fluorescence spectra were recorded in the range of 275–440 nm upon excitation at 270 nm at 25°C. Excitation and emission slits widths were 5/5 nm. The changes in the emission spectra of PGM at a constant concentration of 0.05 mg/ml were monitored in titration series with a gradual increase in concentration (0, 0.17, 0.33, 0.5, 0.66, 0.83, 1 μM) of the added caffeine, **VC5**, **VC5**–caffeine, **VC10**, **VC10**–caffeine, **AC10**, or **AC10**–caffeine. Binary systems (**VC5**–caffeine, **VC10**–caffeine, and **AC10**–caffeine) were taken in equimolar ratio.

2.2.3. UV-Vis Spectroscopy

The UV-Vis spectra were recorded on Spectrophotometer Specord 250 Plus (Analytik Jena AG, Germany) at 25°C. Measurements were carried out in quartz cells with pathway lengths l = 1.0. The UV measurements were in the range of 200–500nm.

2.2.4. Dynamic light scattering

The size of the aggregates was determined by dynamic light scattering on a Zetasizer Nano instrument (Malvern Instruments, UK). The source of laser radiation was a He-Ne gas laser with a power of 4 mW and a wavelength of 632.8 nm. The temperature of the scattering cell was maintained at 25 °C. Each sample was measured three times and the particle size distribution was recorded. Values reported as mean ± standard deviation of the experimental triplicates.

All scatter data were processed using Malvern Zetasizer software.

2.2.5. Preparation of PGM samples

The PGM aqueous solution was prepared by adding PGM to deionized water in a concentration of 0.05 mg/mL (for fluorescence spectroscopy) and 1 mg/mL (for turbidimetry). The dispersion was stirred for 2 h and sonicated for 10 min at room temperature. The PGM dispersion with a concentration of 1 mg/mL was additionally centrifuged for 5 min at 1000 rpm. The

supernatant was recovered and used in experiments. All PGM dispersions were freshly prepared before each experiment.

2.2.6. Turbidimetric titration

The interactions between PGM and calix[4]resorcinols **VC5**, **VC10**, **AC10** in the absence and in the presence caffeine were investigated by turbidimetric titration according to[21]. The solution of 1mg/mL calix[4]resorcinol or 1mg/mL calix[4]resorcinol–0.6 mM caffeine (equimolar ratio) were added to 1mg/mL of the PGM dispersion stepwise and the turbidity (absorption, A) of the samples was measured after each step by UV-Vis spectrophotometer at a wavelength λ=500 nm. A turbidimetric study of the interaction of calix[4]resorcinol **VC5** or **VC10** with calix[4]resorcinol **AC10** was carried out as follows: to a solution of **VC5** or **VC10** (0.1 mM) in water was added an aqueous solution of **AC10** (1 mM) stepwise and the turbidity (absorption, A) of the samples was measured after each step by UV-Vis spectrophotometer at a wavelength λ=500 nm. All experiments were repeated in triplicate and the turbidity values are reported as mean ± standard deviation of the experimental triplicates.

3. Results and discussion

The choice of viologen derivatives carrying a positive charge was guided by the fact that sialic acids have a negative charge at neutral pH values and is present as a monosaccharide fragment in mucins of epithelial tissue.[22] It can be assumed that the viologen groups of calix[4]resorcinol can interact with mucin through electrostatic interactions. Acetate derivative of calix[4]resorcinol can act as hydrogen bond acceptors when interacting with hydroxyl groups[23] in the saccharide moieties of mucin. Moreover, calix[4]resorcinol derivatives perfectly bind metal ions[24], and according to the principle of hard and soft acids and bases[25], the acetate groups have a high affinity for calcium ions.

3.1. Complexation of macrocycles with caffeine and calcium chloride. To establish the possibility of complexation of viologen calix[4]resorcinols (**VC5**, **VC10**) and acetate decyl calix[4]resorcinol **AC10** with caffeine and $CaCl_2$, ^1H NMR spectra of double calix[4]resorcinol–caffeine systems and ternary calix[4]resorcinol–caffeine–$CaCl_2$ systems at ratios of 1:1 and 1:1:10, respectively, were recorded. Viologen calix[4]resorcinols **VC5**, **VC10** in D_2O have acidic pH values of 3.8 and 3.4, respectively, and the addition of caffeine to the solutions of these macrocycles caused a slight increase in pH by 0.5 units to 4.3 and 3.9, respectively. According to the literature data[26], caffeine is in a neutral form at 4 <pH <10, therefore, in order to exclude the effect of its protonation on changes in chemical shifts in NMR spectra, for systems with viologen calix[4]resorcinols, we used a phosphate buffer, which maintained a pH level of 7.4 in solutions. These conditions allow us to compare NMR spectra with each other, and the change in the chemical shifts of protons can only

be attributed to the process of complexation. Acetate calix[4]resorcinol **AC10**, binary **AC10**–caffeine, and ternary **AC10**–caffeine–$CaCl_2$ systems in D_2O have a pH of 8.4, which makes it possible to analyze the changes in chemical shifts of protons in their spectra without using a buffer.

In the ^{1}H NMR spectrum of the binary system of viologen calix[4]resorcinol **VC5** with caffeine, the maximum changes in chemical shifts were recorded for methylene protons H10 in the alkyl fragments of calix[4]resorcinol adjacent to the bridging methylene proton by ~0.06 ppm, while the chemical shifts of the caffeine protons change insignificantly (Figure S1). In contrast to previous studies focused on the complexation between caffeine and calix[4]resorcinols with various alkyl (ethyl-, propyl-, nonyl-) fragments[27], the chemical shifts in the spectrum of binary system relative to individual ones is probably associated with the complexation of caffeine with a calixarene **VC5** due to CH-π-interaction between methylene fragments of the macrocycle and aromatic rings of caffeine. It should be noted that in ref[28], the formation of a complex was observed due to the partial inclusion of the methyl group of caffeine in the cavity of the macrocycle and multiple hydrogen bonds between the carbonyl oxygen atoms of caffeine and the hydroxyl groups of the macrocycles, while the alkyl chains did not participate in the complexation. Probably, the absence of hydroxyl groups in the structure of **VC5** leads to the binding of caffeine by the lower rim alkyl chains near the bridging methylene proton. Considering the literature data for calix[4]resorcinol with pentyl tails on the lower rim[29–32], these macrocycles are characterized by the formation of supramolecular head-to-tail aggregates. In our case, the aggregates of **VC5** retain their morphology upon binding with caffeine, which is reflected in downfield shift of the protons of the pentyl chain.

In the ternary **VC5**–caffeine–$CaCl_2$ system, the signals of methylene proton H10 and terminal methyl proton H14 in the alkyl fragments of calixarene **VC5** are shifted downfield by ~0.04 ppm and ~0.02 ppm, respectively. The changes in the proton chemical shifts of viologen fragments of **VC5** and caffeine are insignificant (by ~0.01 ppm). Nevertheless, based on changes in the chemical shifts of **VC5** in the presence of caffeine and calcium chloride, it can be assumed that the macrocycle–caffeine complex interacts with calcium ions. The binding of calcium ions can be realized due to bridging oxygen atoms or cation-π-interaction with aromatic fragments[33].

According to dynamic light scattering (DLS) measurements the individual caffeine molecules do not form aggregates in aqueous solution. The molecules of **VC5** with the concentration of 1 mM form large aggregates of ~319±8 nm (Figure S2), which are organized in a manner of head-to-tail orientation and morphology[32]. The addition of 1 mM caffeine to 1 mM calix[4]resorcinol **VC5** does not lead to any noticeable changes in the particle size distribution compared to individual **VC5**, which indicates the preservation of the structure of aggregates in binary system. The DLS data for ternary **VC5**–caffeine–$CaCl_2$ system also show the unimodal

distribution of particles with an average size of ~305±18 nm. Thus, the changes revealed in the chemical shifts in the NMR spectra for these systems indicate the interaction of **VC5** with caffeine and their complex with calcium ions, which are not accompanied by the destruction of mixed aggregates.

In the case of viologen calix[4]resorcinol with decyl fragments **VC10**, the binding with caffeine was not observed. In the spectrum of the binary **VC10**–caffeine system the changes of chemical shifts are insignificant. However, in the ternary **VC10**–caffeine–$CaCl_2$ system, a shift of the bridging protons H7 by ~0.04 ppm is observed, which is obviously due to the binding of calcium ions by oxygen-containing bridging fragments of the macrocycle. In the system with macrocycle **VC5** this proton changes by only ~0.01 ppm, which indicates the better binding capacity of **VC10** with respect to calcium ions. The weaker binding of calcium ions by calix[4]resorcinol with pentyl fragments **VC5** may be due to the above mentioned ability of **VC5** to form head-to-tail aggregates, when alkyl tails enter the calixarene cavity of an adjacent molecule, thereby preventing the complexation of bridging oxygen with calcium. Macrocycle **VC10** with decyl fragments at a concentration above 0.2 mM forms vesicular particles, where hydrophobic interactions prevail[32]; therefore, bridging oxygen does not have steric hindrances to binding metal ion.

The decyl derivative **VC10** and its binary system with caffeine form large aggregates with an average size of ~250±57 and 308±37 nm, respectively, similar to calix[4]resorcinol with pentyl fragments **VC5**. However, the addition of a ten-fold excess of calcium in the ternary system leads to a sharp decrease in particle size to ~4±0.2 nm and a slight decrease in the polydispersity index (from 0.461 to 0.397), which differs significantly from the results for the ternary **VC5**–caffeine–$CaCl_2$. The decrease in particle size is apparently caused by the binding of calcium to calix[4]resorcinol **VC10** and the destruction of large aggregates. The vesicular structure of **VC10** aggregates is the most preferable for binding calcium ions due to the steric accessibility of bridging oxygen atoms. The binding of calcium to **VC10** causes significant disruption of aggregates, which correlates with NMR spectroscopy data for the ternary **VC10**–caffeine–$CaCl_2$ system where a noticeable chemical shift of H7 protons was observed in contrast to the binary system. Thus, the hydrophobicity of viologen calix[4]resorcinol cavitands determines not only the morphology of the aggregates they form, but also their ability to bind calcium ions, which depends on the shape of the aggregates. The stacking model of self-assembly sterically hinders the pathway of calcium ions to the upper rim, namely to the bridging oxygen atoms. The shape of the vesicular aggregates with alkyl tails inside the bilayer and headgroups oriented towards the aqueous phase favors metal binding. However, when calcium chloride is added to the spherical aggregates of **VC10**, not only calcium ions, but also its counterpart chloride, which can electrostatically compensate positively

charged viologen groups, is involved in binding with **VC10**, resulting either in the destruction of aggregates or their morphological rearrangement.

For the system of acetate decyl calix[4]resorcinol **AC10** with caffeine in the NMR spectrum, the maximum change in chemical shifts compared to the spectra of individual compounds is observed for the proton signals of alkyl fragments of calix[4]resorcinol **AC10** and methyl proton of caffeine H2 by ∼0.03 ppm (Figure S5). In addition, the signals of H1, H3, and H5 of macrocycle **AC10** are shifted by ∼0.02 ppm. Thus, the caffeine molecule can interact with the viologen derivatives **VC5** and **VC10**, as well as acetate derivative of calix[4]resorcinol **AC10**, but the revealed relatively small changes in chemical shifts in the NMR spectra of binary systems indicate their weak interaction, which does not allow us to determine the stoichiometry of complexes between macrocycles and caffeine by the Job method. Further study of ternary system of macrocycle **AC10** with caffeine and a ten-fold excess of calcium chloride showed that in contrast to viologen macrocycles, the acetate derivative of calix[4]resorcinol **AC10** form a strong complex with $CaCl_2$, which precipitate within a few hours in NMR tube (Figure S6). The NMR spectrum of the ternary system shows only the presence of caffeine signals in the solution (Figure S5), which means the entire amount of calix[4]resorcinol **AC10** in a complex with $CaCl_2$ is precipitated. It is known that acetate derivatives are able to form complexes with alkali metals, in which a metal is involved in bidentate chelate $O_{carboxy}$, $O_{phenoxy}$ interactions[34,35]. Apparently, the presence of eight chelating functional groups in one molecule determines the high binding capacity of calix[4]resorcinol **AC10** towards calcium ions.

In contrast to viologen derivatives, acetate calix[4]resorcinol **AC10** at the same concentration forms much smaller aggregates with a diameter of ∼68±1 nm (Figure S7). With the addition of caffeine, particles are enlarged to ∼106±27 nm, which indicates that interaction between **AC10** aggregates and caffeine results in larger co-aggregates. The size in the ternary **AC10**–caffeine–$CaCl_2$ system was not measured due to its precipitation.

3.2. Interaction with mucin. It is well known that mucins are mixtures of carbohydrate-protein compounds secreted by the epithelial cells of the mucous membranes of various (respiratory, digestive, urogenital) tracts, as well as of the submandibular and sublingual salivary glands. The mucoadhesive properties of viologen calixarenes **VC5**, **VC10**, and acetate calixarene **AC10** in the presence of caffeine were evaluated by studying the interaction with mucin (porcine gastric mucin, PGM) in aqueous solutions. Commercial PGM is widely used as a model mucin[21,36–40] due to the similarities between porcine and human intestinal mucin[41]. PGM consists of both MUC5AC and MUC6 and is commonly used to mimic human saliva mucins (MUC5B). The fluorescence spectroscopy is one of the most common methods for studying the physicochemical properties of proteins[42]. The fluorescence properties of proteins are primarily due to tryptophan residues. The

fluorescence emission of tryptophan is very sensitive to the changes in its microenvironment, especially polarity. In accordance with this, the complexation with low molecular weight molecules and macromolecules significantly affects the fluorescence spectra of proteins. In order to minimize the inner filter effect on steady state fluorescence spectra, the maximum concentration of the investigated compounds was chosen so that the absorption in the UV spectra was ~0.1 (Figure 2). Under these conditions, the fluorescence intensity is constant at each point along the light path and there is no concentration quenching effect of the compounds on the emission spectra[43].

PGM alone shows a strong fluorescence emission at 350 nm after excitation at 270 nm which is mainly due to the presence of tryptophan residues. The addition of caffeine at various concentrations to the PGM at a constant concentration did not lead to a noticeable change in the emission intensity in the fluorescence spectra. (Figure 3a). However, in the presence of **VC5**–caffeine or **VC10**–caffeine complex, a significant decrease in the peak maximum was observed (Figure 3c, e), which indicates the interaction of the binary system with PGM. As in[42], it can be assumed that upon binding to mucin, the **VC5**–caffeine and **VC10**–caffeine systems change the microenvironment of tryptophan, which leads to the quenching of PGM fluorescence intensity. Similarly, the fluorescence intensity of PGM gradually decreased in the presence of viologen calix[4]resorcinols **VC5** or **VC10** alone (Figure 3b, d).The addition of acetate calix[4]resorcinol **AC10** alone and in a complex with caffeine at various concentrations to PGM at a constant concentration resulted in the bathochromic shift with an increase in emission intensity (Figure 3f, g). Thus, calixarenes **VC5**, **VC10**, and **AC10** themselves interact with mucin strongly and, in combination with a drug, the system exhibits also mucoadhesive properties.

Another widely used and reliable method for studying mucoadhesive interactions is turbidimetry, based on the change in the light intensity when passing through a suspension of particles[44]. The study of the interaction of viologen and acetate derivatives of calix[4]resorcinols **VC5**, **VC10**, and **AC10** with PGM was also carried out using turbidimetric titration, when the mucin solution was titrated with a macrocycle solution or binary macrocycle–caffeine (1:1) system. The turbidity of solutions at various ratios was measured using a UV spectrophotometer at 500 nm, because at this wavelength there are no absorption bands of calixarenes and caffeine (Figure 2).

According to turbidimetric data, viologen calixarenes **VC5**, **VC10** and their binary systems with caffeine show good binding to mucin (Figure 4). The addition of caffeine practically does not affect the mucin binding. The mucin titration with calix[4]resorcinols **VC5**, **VC10** and their mixtures with caffeine have one maximum on the turbidity curve at almost the same mass ratio of [calixarene]/[mucin] ~0.25–0.3. This indicates that viologen calixarenes **VC5**, **VC10** and their

complexes with caffeine are able to bind to mucin due to the electrostatic interaction of positively charged viologen groups and negatively charged sulfated glycans and sialic acid residues in mucin. With an increase in the concentration of the viologen macrocycle, the aggregation of mucin particles is observed first, which is reflected in an increase of absorption, and then, a further increase in the macrocycle concentration, on the contrary, leads to a decrease of absorption and disaggregation[21].

The turbidimetric titration curves for acetate decyl calixarene **AC10** and binary **AC10**–caffeine system did not reveal any interaction with mucin (Figure 4). The difference with the fluorescence spectroscopy data is due to the fact that turbidimetry method is more suitable for studying catanionic mixtures. Additionally, we decided to check the supramolecular interaction between mucin and **AC10** using NMR diffusion measurements. As previously shown[17–19], NMR-self-diffusion technique (Fourier transform pulsed-gradient spin-echo (FT-PGSE) experiment) is sensitive to the formation of aggregates and very powerful method for screening drugs and characterizing their binding properties. The FT-PGSE experiment was used to determine the self-diffusion coefficient (D_s) of the components in both individual and mixed systems. Table 1 shows that D_s of calix[4]resorcinol **AC10** decreases by 28% in the presence of mucin, which indicates their binding. At the same time, it was not possible to determine D_s of mucin in binary **AC10**–mucin and ternary **AC10**–caffeine–mucin mixtures due to the overlapping of signals of the mucin and macrocycle. However, it was possible to determine D_s of caffeine in ternary **AC10**–caffeine–mucin system which is reduced in comparison with the self-diffusion of individual caffeine. The self-diffusion of caffeine also decreases in a mixture with **AC10**, indicating the complex formation between them. In addition, D_s of **AC10** does not decrease in the binary **AC10**–caffeine and ternary **AC10**–caffeine–mucin systems. Thus, based on NMR-diffusion data, it can be assumed that **AC10** binds to mucin and efficiently interacts with caffeine, but caffeine binding prevents macrocycle **AC10** from interacting with mucin.

The diffusion experiments for systems with viologen calix[4]resorcinols **VC5**, **VC10** confirmed the interaction with mucin, which is in accordance with turbidimetric data. A significant decrease in D_s of mucin by $0.77 \cdot 10^{-10}$, m^2/s was observed in the binary **VC5**–mucin system (Table 1). It was not possible to determine D_s of mucin in **VC10**–mucin mixture due to the overlap of many peaks of mucin with the peaks of macrocycle and caffeine. 1H NMR spectra of these systems have broad overlapped peaks and the signals of the mucin are disappeared in FT-PGSE spectra. This phenomenon may be due to the several factors, mainly, very short transverse relaxation times of the molecules and the exchange between the different positions of components in the binding site. In addition, a decrease in D_s of caffeine is observed in binary **VC5**/**VC10**–caffeine and ternary **VC5**/**VC10**–caffeine–mucin systems, which indicates the binding of caffeine in the systems. D_s of

caffeine in the ternary mixture with **VC5**/**VC10** and mucin is lower than in the binary mixture with the macrocycle, which probably indicates the competitive binding of mucin and caffeine with the viologen macrocycles, and **VC5** and **VC10** molecules bind somewhat more to mucin.

3.3. Investigation of mixed systems based on viologen and acetate derivatives of calix[4]resorcinol. Taking into account that the acetate decyl calixarene **AC10** binds calcium ions well, and the viologen calixarenes **VC5** and **VC10** are capable of binding to mucin, we assumed that the mixing of two different calix[4]arene derivatives would combine these two binding properties in one system. When **VC5** or **VC10** is mixed with **AC10** in a 1:1 ratio, the solution becomes cloudy and a precipitate appears. In NMR spectra with such a ratio, no signals are observed, and a broad hump in a strong field (0 to 1.5 ppm) is recorded. The positively charged viologen groups of **VC5** and **VC10** may interact electrostatically with the negatively charged acetate groups to form a complex. The positive charge is completely compensated at an equimolar ratio, and it is necessary to give the system a positive charge in order to bind to mucin. In this regard, systems with a two-fold excess of viologen calixarenes were prepared. In the NMR spectrum of binary **VC5**:**AC10** system with 2:1 ratio, the signals of only the viologen calixarene **VC5** is recorded with a slight shift of proton signals to ~0.03 ppm in comparison with the spectrum of individual **VC5** (Figure S8).

^{1}H NMR signals of calixarene **VC10** are strongly downshifted in binary **VC10**–**AC10** system with 2:1 ratio as compared to the spectrum of individual **VC10** (Figure S9). The maximum shift is observed for bridging H7 protons by ~0.18 ppm, H11-H18 protons of the decyl fragments by ~0.13 ppm, and methylene protons H6 by ~0.08 ppm, which indicates binding by both the charged viologen group and the lower rim due to hydrophobic interactions between the alkyl fragments of the calixarenes **VC10** and **AC10**. The stronger chemical shifts of protons for **VC10** as compared to **VC5** indicates the cooperative effect of hydrophobic and electrostatic interactions in the complexation of viologen decyl calix[4]resorcinol **VC10** with acetate decyl calix[4]resorcinol **AC10**.

Further, the turbidimetric titration curves of **VC5** and **VC10** by **AC10** in water were plotted (Figure 5), which confirm the formation of joint complexes with stoichiometry 1:1 (calix[4]resorcinol **VC5**–calix[4]resorcinol **AC10**) and 2:3 (calix[4]resorcinol **VC10**–calix[4]resorcinol **AC10**). It is interesting to note that the maximum absorption intensity for **VC10**–**AC10** system is almost twice as large as that for **VC5**–**AC10** system, which means a stronger interaction of **AC10** with **VC10** when compared with **VC5**. Thus, the hydrophobicity of the lower rim of viologen calixarenes determines the ability to interact with oppositely charged amphiphilic **AC10**, i.e., the longer the alkyl chains of viologen calixarene, the more effective is

the interaction. This result indicates the importance of the hydrophobicity of amphiphilic building blocks of macrocyclic nature in the design of joint aggregates.

Afterwards, we decided to investigate the ability of mixed systems of **VC5** and **VC10** with **AC10** to interact with mucin in an aqueous medium, but during the turbidimetric titration of mucin with a mixture of calixarenes, a precipitate gradually formed, which does not allow us to determine the absorption intensity at 500 nm correctly. Nevertheless, the presence of a precipitate in the mixture of calix[4]resorcinols with mucin indicates the interaction of viologen macrocycles with mucin, despite the joint aggregation with acetate calixarene. To reveal the possibility of calcium binding by a mixture of viologen and acetate calix[4]resorcinols, the turbidimetric titration of their mixtures with calcium chloride also was performed. However, the addition of calcium chloride to the mixtures of viologen macrocycles **VC5**, **VC10** with acetate calixarene **AC10** led to the formation of a precipitate, and the titration curves were not reproduced. It should be noted that, the greater the proportion of **AC10** in the binary mixture, the more precipitate was formed. Thus, acetate calixarene **AC10** in a complex with viologen calixarenes **VC5**, **VC10** retains its binding capacity for calcium.

As mentioned above, the equimolar mixtures of **VC5** and **VC10** with **AC10** are very unstable in an aqueous medium and precipitate. To give the system stability and a positive charge for binding to mucin further we investigated mixed compositions with two and threefold excess of viologen calixarenes. The sizes of mixed systems based on viologen and acetate derivatives of calix[4]resorcinol were measured by DLS over time (Figure 6). In binary systems of **AC10** with **VC5** and **VC10**, regardless of the ratio of the components, a high-quality correlation function was detected (Figure S10-S13), which probably indicates a spherical shape of the aggregates. Considering the literature data on catanionic mixtures of amphiphiles, it can be assumed that aggregates of a vesicular shape are formed in the samples studied. The stability of the mixtures was evaluated for almost a month when stored at room temperature, and Figure 6 shows that the size of the aggregates **VC10**–**AC10** does not change in the aqueous medium significantly. The stability of this system can be caused by additional hydrophobic interactions of decyl chains of calix[4]resorcinols **VC10** and **AC10**, which once again indicates the importance of the hydrophobic component in the formation of stable amphiphilic structures.

4. Conclusions

This is the first research attempt to elucidate the mucoadhesive properties of calixarene derivatives. Apparently, for successful interaction with mucin the supramolecular system based on calixarenes presumably should be multitarget, and therefore this system should contain both cationic and anionic fragments. The cationic moiety in viologen calix[4]resorcinol is mainly responsible for the

interaction with mucin, and the anionic groups in acetate calix[4]resorcinol are responsible for the extraction of calcium ions, which will facilitate the permeability of a drug through the epithelial cells. The main feature of amphiphilic calixarenes used in this work is their spontaneous self-assembly due to non-covalent association, which reduces synthetic efforts in the preparation of useful nanoobjects with several binding sites. The complexation between viologen and acetate derivatives of calix[4]resorcinol was achieved by simple mixing of two compounds in water. The complexes can self-assemble into spherical particles of likely biomimetic vesicular shape. The dependences of turbidimetric titration have shown the strong electrostatic interaction between the viologen calix[4]resorcinol **VC10** and acetate calix[4]resorcinol **AC10** with porcine gastric mucin. The weaker interaction between calix[4]resorcinols **VC5** and **AC10** indicates that the hydrophobicity of the lower rim of viologen calixarenes determines the ability to interact with oppositely charged acetate calixarene **AC10**, i.e., the longer the alkyl chains of viologen calixarene, the more effective is the interaction with long-chain amphiphile and the more stable the joint aggregates. The acetate calixarene **AC10** in a complex with viologen calixarenes **VC5**, **VC10** retains its binding capacity for calcium ions, while **VC5** and **VC10** in a complex with **AC10** are able to maintain interaction with mucin. These results revealed strong affinity of calixarenes to mucin and enrich the library of mucoadhesive compounds for the development of potential dosage forms.

Funding

This research was funded by Russian Science Foundation, grant number 19-73-30012. Authors thank the Assigned Spectral-Analytical Center of FRC Kazan Scientific Center of RAS.

Declaration of competing interest

The authors have no conflict of interest to declare.

Appendix A. Supplementary data

Supplementary data to this article can be found online at

References

[1] V. V. Khutoryanskiy, Beyond PEGylation: Alternative surface-modification of nanoparticles with mucus-inert biomaterials, Adv. Drug Deliv. Rev. 124 (2018) 140–149. https://doi.org/10.1016/j.addr.2017.07.015.

[2] R.P. Brannigan, V. V. Khutoryanskiy, Progress and Current Trends in the Synthesis of Novel Polymers with Enhanced Mucoadhesive Properties, Macromol. Biosci. 19 (2019) 1–

11. https://doi.org/10.1002/mabi.201900194.

[3] T.M.M. Ways, K.W. Ng, W.M. Lau, V. V. Khutoryanskiy, Silica nanoparticles in transmucosal drug delivery, Pharmaceutics. 12 (2020) 1–25. https://doi.org/10.3390/pharmaceutics12080751.

[4] L. Liu, C. Tian, B. Dong, M. Xia, Y. Cai, R. Hu, X. Chu, Models to evaluate the barrier properties of mucus during drug diffusion, Int. J. Pharm. 599 (2021) 120415. https://doi.org/10.1016/j.ijpharm.2021.120415.

[5] S. Alaei, H. Omidian, Mucoadhesion and Mechanical Assessment of Oral Films, Eur. J. Pharm. Sci. 159 (2021) 105727. https://doi.org/10.1016/j.ejps.2021.105727.

[6] P.W.J. Morrison, N.N. Porfiryeva, S. Chahal, I.A. Salakhov, C. Lacourt, I.I. Semina, R.I. Moustafine, V. V. Khutoryanskiy, Crown Ethers: Novel Permeability Enhancers for Ocular Drug Delivery?, Mol. Pharm. 14 (2017) 3528–3538. https://doi.org/10.1021/acs.molpharmaceut.7b00556.

[7] M.A. Heinrich, B. Martina, J. Prakash, Nanomedicine strategies to target coronavirus, Nano Today. 35 (2020) 100961. https://doi.org/10.1016/j.nantod.2020.100961.

[8] P. Neri, J.L. Sessler, M.-X. Wang, eds., Calixarenes and Beyond, Springer, 2016. https://doi.org/10.1007/978-3-319-31867-7_34.

[9] C.D. Gutsche, Calixarenes Revisited, Royal Society of Chemistry: Cambridge, UK, 1998.

[10] V. Böhmer, Calixarenes, Macrocycles with (Almost) Unlimited Possibilities, Angew. Chemie Int. Ed. English. 34 (1995) 713–745. https://doi.org/10.1002/anie.199507131.

[11] R. Kumar, A. Sharma, H. Singh, P. Suating, H.S. Kim, K. Sunwoo, I. Shim, B.C. Gibb, J.S. Kim, Revisiting Fluorescent Calixarenes: From Molecular Sensors to Smart Materials, Chem. Rev. 119 (2019) 9657–9721. https://doi.org/10.1021/acs.chemrev.8b00605.

[12] D.J. Cram, S. Karbach, H.-E. Kim, C.B. Knobler, E.F. Maverick, J.L. Ericson, R.C. Helgeson, ChemInform Abstract: Host-Guest Complexation. Part 46. Cavitands as Open Molecular Vessels Form Solvates., ChemInform. 19 (1988) 2229–2237. https://doi.org/10.1002/chin.198829113.

[13] R. Kashapov, G. Gaynanova, D. Gabdrakhmanov, D. Kuznetsov, R. Pavlov, K. Petrov, L. Zakharova, O. Sinyashin, Self-assembly of amphiphilic compounds as a versatile tool for construction of nanoscale drug carriers, Int. J. Mol. Sci. 21 (2020) 1–47. https://doi.org/10.3390/ijms21186961.

[14] L. Mahlert, J. Anderski, D. Mulac, K. Langer, The impact of gastrointestinal mucus on nanoparticle penetration – in vitro evaluation of mucus-penetrating nanoparticles for photodynamic therapy, Eur. J. Pharm. Sci. 133 (2019) 28–39. https://doi.org/10.1016/j.ejps.2019.03.010.

[15] A.Y. Ziganshina, S. V. Kharlamov, D.E. Korshin, R.K. Mukhitova, E.K. Kazakova, S.K. Latypov, V. V. Yanilkin, A.I. Konovalov, Electrochemical behaviour of a molecular capsule based on methylviologen-resorcinarene and sulfonatomethylene-resorcinarene, Tetrahedron Lett. 49 (2008) 5312–5315. https://doi.org/10.1016/j.tetlet.2008.06.084.

[16] T.Y. Sergeeva, I.R. Nizameev, K. V. Kholin, M.K. Kadirov, A.I. Samigullina, A.T. Gubaidullin, R.K. Mukhitova, A.Y. Ziganshina, I.S. Antipin, Polymer and supramolecular nanocontainers based on carboxylate derivatives of resorcinarenes for binding of substrates and design of composites for catalysis, Russ. Chem. Bull. 69 (2020) 351–359. https://doi.org/10.1007/s11172-020-2767-x.

[17] P. Stilbs, Fourier transform pulsed-gradient spin-echo studies of molecular diffusion, Prog. Nucl. Magn. Reson. Spectrosc. 19 (1987) 1–45. https://doi.org/10.1016/0079-6565(87)80007-9.

[18] Y. Cohen, L. Avram, L. Frish, Diffusion NMR spectroscopy in supramolecular and combinatorial chemistry: an old parameter–new insights, Angew. Chem. Int. Ed. Engl. 44 (2005) 520–554. https://doi.org/10.1002/anie.200300637.

[19] T. Brand, E.J. Cabrita, S. Berger, Intermolecular interaction as investigated by NOE and diffusion studies, Prog. Nucl. Magn. Reson. Spectrosc. 46 (2005) 159–196. https://doi.org/10.1016/j.pnmrs.2005.04.003.

[20] D. Wu, A. Chen, Jr.,C.S. Johnson, An improved diffusion-ordered spectroscopy experiment incorporating bipolar-gradient pulses, J. Magn. Reson., Ser. A. 115 (1995) 260–264. https://doi.org/10.1006/jmra.1995.1176.

[21] I.A. Sogias, A.C. Williams, V. V. Khutoryanskiy, Why is chitosan mucoadhesive?, Biomacromolecules. 9 (2008) 1837–1842. https://doi.org/10.1021/bm800276d.

[22] V. V. Khutoryanskiy, Advances in Mucoadhesion and Mucoadhesive Polymers, Macromol. Biosci. 11 (2011) 748–764. https://doi.org/10.1002/mabi.201000388.

[23] Z. Slim, M. Jancheva, S. Grigorakis, D.P. Makris, Polyphenol extraction from Origanum dictamnus using low-transition temperature mixtures composed of glycerol and organic salts: Effect of organic anion carbon chain length, Chem. Eng. Commun. 205 (2018) 1494–1506. https://doi.org/10.1080/00986445.2018.1458026.

[24] S.N. Podyachev, N.E. Burmakina, V. V. Syakaev, S.N. Sudakova, R.R. Shagidullin, A.I. Konovalov, Synthesis, IR and NMR characterization and ion extraction properties of tetranonylcalix[4]resorcinol bearing acetylhydrazone groups, Tetrahedron. 65 (2009) 408–417. https://doi.org/10.1016/j.tet.2008.10.008.

[25] R.G. Pearson, Hard and soft acids and bases, HSAB, part I: Fundamental principles, J. Chem. Educ. 45 (1968) 581–587. https://doi.org/10.1021/ed045p581.

[26] T. Katsu, Y. Tsunamoto, N. Hanioka, K. Komagoe, K. Masuda, S. Narimatsu, A caffeine-sensitive membrane electrode: Previous misleading report and present approach, Anal. Chim. Acta. 620 (2008) 50–54. https://doi.org/10.1016/j.aca.2008.05.027.

[27] Lyondellbasell, Spheripol process description, (n.d.). www.lyondellbasell.com.

[28] P. Thuéry, M. Nierlich, Z. Asfari, J. Vicens, O. Morikawa, H. Konishi, Crystal Structure of C-(n-propyl)calix[4]resorcinarene and its Complex with Caffeine, Supramol. Chem. 13 (2001) 521–527. https://doi.org/10.1080/10610270108028298.

[29] C. Aakeröy, N. Schultheiss, J. Desper, Synthesis and hydrogen-bond capabilities of an amino-pyridine functionalized cavitand, CrystEngComm. 9 (2007) 211–214. https://doi.org/10.1039/b618728e.

[30] V. V. Syakaev, A.R. Mustafina, J.G. Elistratova, S.K. Latypov, A.I. Konovalov, Head-to-tail aggregates of sulfonatomethylated calix[4]resorcinarene in aqueous solutions, Supramol. Chem. 20 (2008) 453–460. https://doi.org/10.1080/10610270701310930.

[31] J.E. Morozova, E.K. Kazakova, D.A. Mironova, Y. V. Shalaeva, V. V. Syakaev, N.A. Makarova, A.I. Konovalov, Investigation of tetramethylenesulfonated calix[4]resorcinarene interactions with azo dyes in aqueous solution, J. Phys. Chem. B. 114 (2010) 13152–13158. https://doi.org/10.1021/jp106060p.

[32] R.R. Kashapov, S. V. Kharlamov, E.D. Sultanova, R.K. Mukhitova, Y.R. Kudryashova, L.Y. Zakharova, A.Y. Ziganshina, A.I. Konovalov, Controlling the size and morphology of supramolecular assemblies of viologen-resorcin[4]arene cavitands, Chem. - A Eur. J. 20 (2014) 14018–14025. https://doi.org/10.1002/chem.201403721.

[33] V.P. Santarelli, A.L. Eastwood, D.A. Dougherty, C.A. Ahern, R. Horn, Calcium block of single sodium channels: Role of a pore-lining aromatic residue, Biophys. J. 93 (2007) 2341–2349. https://doi.org/10.1529/biophysj.107.106856.

[34] G. Smith, D.E. Lynch, Two-dimensional coordination polymeric structures in caesium complexes with ring-substituted phenoxyacetic acids, Acta Crystallogr. Sect. C Struct. Chem. 70 (2014) 606–612. https://doi.org/10.1107/S2053229614010596.

[35] G. Smith, Two-dimensional coordination polymeric structures in the sodium, potassium and rubidium complex salts with (4-fluorophenoxy)acetic acid, Acta Crystallogr. Sect. C Struct. Chem. 73 (2017) 979–983. https://doi.org/10.1107/S2053229617014103.

[36] N. A. Fefelova, Z. S. Nurkeeva, G. A. Mun, V. V. Khutoryanskiy, Mucoadhesive interactions of amphiphilic cationic copolymers based on [2-(methacryloyloxy)ethyl]trimethylammonium chloride, Int. J. Pharm. 339 (2007) 25–32. https://doi:10.1016/j.ijpharm.2007.02.019.

[37] B. Menchicchi, J. P. Fuenzalida, K. B. Bobbili, A. Hensel, M. J. Swamy, F. M. Goycoolea,

Structure of chitosan determines its interactions with mucin, Biomacromolecules. 15 (2014) 3550−3558. https://doi.org/10.1021/bm5007954.

[38] E. D. H. Mansfield, K. Sillence, P. Hole, A. C. Williams, V. V. Khutoryanskiy, POZylation: a new approach to enhance nanoparticle diffusion through mucosal barriers, Nanoscale. 7 (2015) 13671–13679. https://doi:10.1039/c5nr03178h.

[39] B. Á. Szilágyi, A. Mammadova, B. Gyarmati, A. Szilágyi, Mucoadhesive interactions between synthetic polyaspartamides and porcine gastric mucin on the colloid size scale Colloids Surf., B. 194 (2020) 111219. https://doi:10.1016/j.colsurfb.2020.111219.

[40] I. M. Hansen, M. F. Ebbesen, L. Kaspersen, T. Thomsen, K. Bienk, Y. Cai, B. M. Malle, K. A. Howard, Hyaluronic acid molecular weight-dependent modulation of mucin nanostructure for potential mucosal therapeutic applications, Mol. Pharm. 14 (2017) 2359–2367. https://doi:10.1021/acs.molpharmaceut.7b00236.

[41] M. Ahmad, C. Ritzoulis, J. Chen, Shear and extensional rheological characterisation of mucin solutions, Colloids Surf., B. 171, (2018) 614–621. https://doi.org/10.1016/j.colsurfb.2018.07.075.

[42] C. Butnarasu, N. Barbero, D. Pacheco, P. Petrini, S. Visentin, Mucin binding to therapeutic molecules: The case of antimicrobial agents used in cystic fibrosis, Int. J. Pharm. 564 (2019) 136–144. https://doi.org/10.1016/j.ijpharm.2019.04.032.

[43] M. Makarska-Bialokoz, Spectroscopic study of porphyrin-caffeine interactions, J. Fluoresc. 22 (2012) 1521–1530. https://doi.org/10.1007/s10895-012-1090-9.

[44] Y.A. Albarkah, R.J. Green, V. V. Khutoryanskiy, Probing the Mucoadhesive Interactions between Porcine Gastric Mucin and Some Water-Soluble Polymers, Macromol. Biosci. 15 (2015) 1546–1553. https://doi.org/10.1002/mabi.201500158.

Figure 1. Chemical structures of viologen derivatives **VC5**, **VC10** and acetate derivative **AC10** of calix[4]resorcinol.

Figure 2. UV-Vis absorption spectra of caffeine, **VC5**, **VC10**, **AC10** at a concentration of 0.001 mM.

Figure 3. Steady state fluorescence spectra of PGM at a constant concentration of 0.05 mg/mL in the presence of caffeine (a), **VC5** (b), **VC5**–caffeine (c), **VC10** (d), **VC10**–caffeine (e), **AC10** (f), and **AC10**–caffeine (g); 25 °C.

Figure 4. Turbidimetric titration of 1 mg/mL PGM with 1 mg/mL solution of calix[4]resorcinols **VC5**, **VC10**, **AC10** in the absence (dash line) and presence (solid line) of 0.6 mM caffeine.

Figure 5. Turbidimetric titration of 0.1 mM **VC5**, 0.1 mM **VC10** by 1 mM **AC10** in aqueous solution.

Figure 6. Particle size distribution of 0.1 mM **VC5**–0.033mM **AC10**, 0.1 mM **VC5**–0.05mM **AC10**, 0.1 mM **VC10**–0.033mM **AC10**, and 0.1mM **VC10**–0.05mM **AC10** in aqueous solutions over time.

Table 1. Self-diffusion coefficients of calix[4]resorcinols (**AC10**, **VC5**, **VC10**), binary calix[4]resorcinol–mucin, calix[4]resorcinol–caffeine and ternary calix[4]resorcinol–caffeine–mucin systems determined by FT-PGSE NMR experiments.

Table 1. Self-diffusion coefficients of calix[4]resorcinols (**AC10**, **VC5**, **VC10**), binary calix[4]resorcinol–mucin, calix[4]resorcinol–caffeine and ternary calix[4]resorcinol–caffeine–mucin systems determined by FT-PGSE NMR experiments.

$D_s \cdot 10^{-10}$, m^2/s								
calix[4]resorcinol **AC10**	caffeine	mucin	calix[4]resorcinol **VC5**	caffeine	mucin	calix[4]resorcinol **VC10**	caffeine	mucin
1.39±0.08	7.71±0.05	2.02±0.13	2.26±0.06	7.71±0.05	2.02±0.13	1.02±0.07	7.71±0.05	2.02±0.13
Binary **AC10**–mucin system			Binary **VC5**–mucin system			Binary **VC10**–mucin system		
1.00±0.09	-	*	2.24±0.10	-	1.25±0.24	0.95±0.09	-	*
Binary **AC10**–caffeine system			Binary **VC5**–caffeine system			Binary **VC10**–caffeine system		
1.41±0.11	6.73±0.09	-	2.25±0.10	7.11±0.10	-	1.01±0.10	7.19±0.09	-
Ternary **AC10**–caffeine–mucin system			Ternary **VC5**–caffeine–mucin system			Ternary **VC10**–caffeine–mucin system		
1.39±0.14	6.67±0.10	*	2.24±0.12	7.21±0.09	*	0.97±0.13	7.40±0.10	*

* impossible to determine D_s of mucin

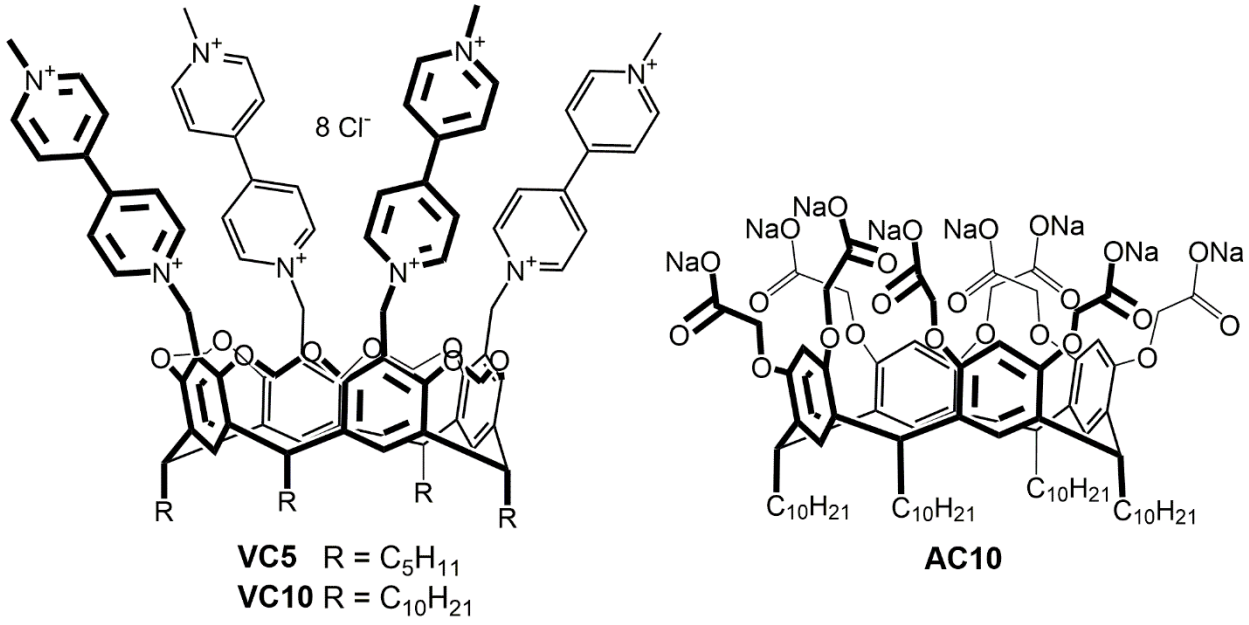

Figure 1

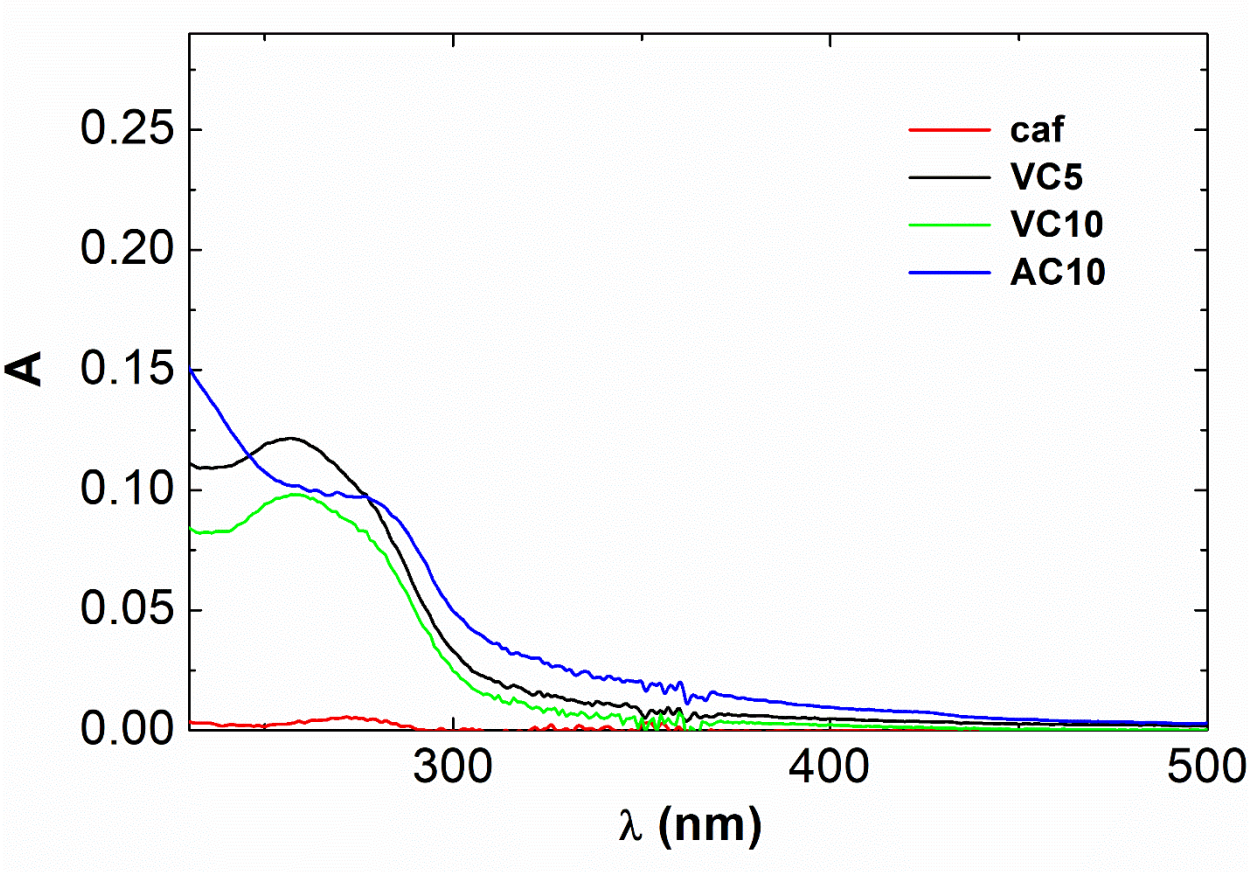

Figure 2

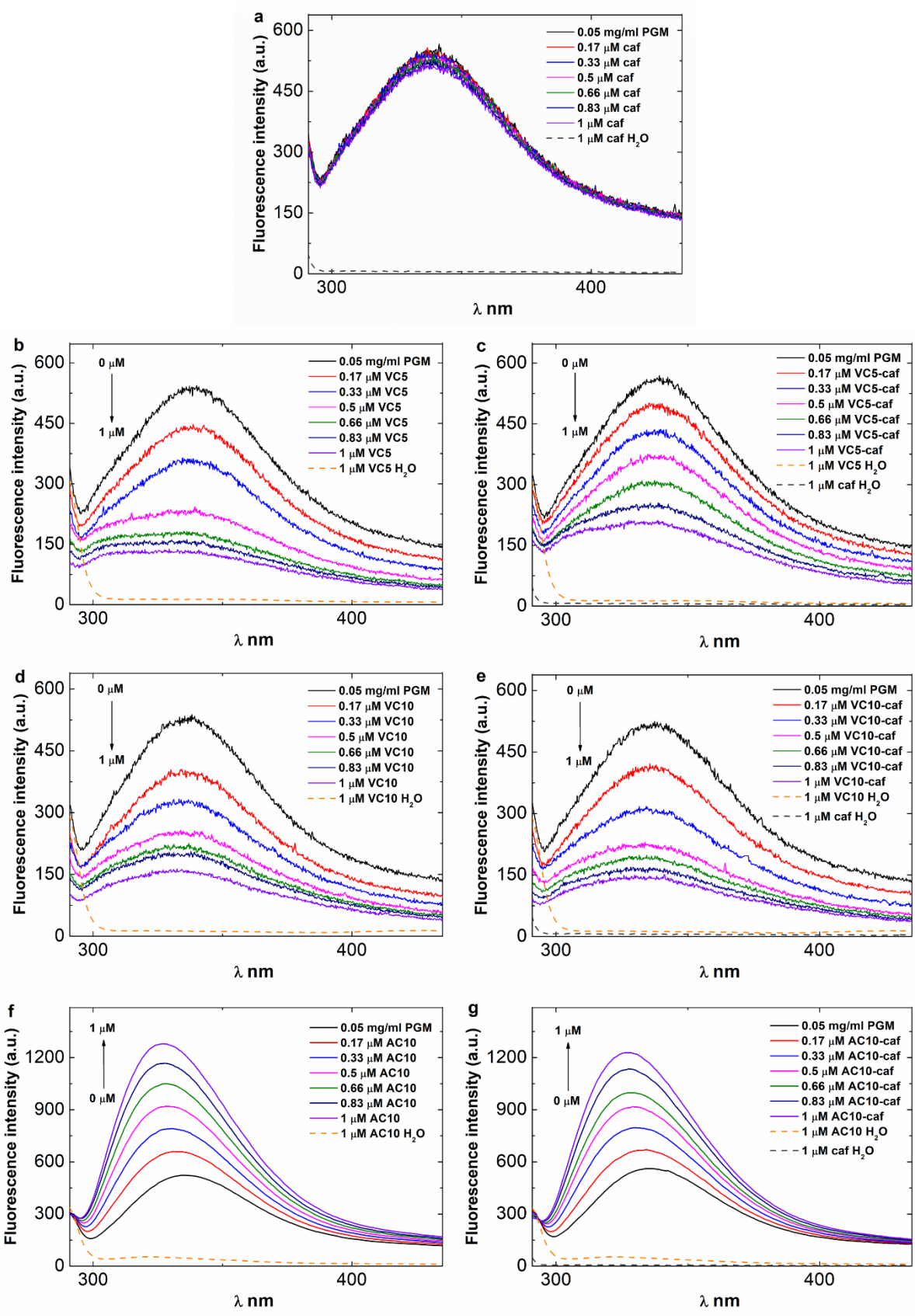
a
Fluorescence intensity (a.u.)
λ nm
0.05 mg/ml PGM
0.17 μM caf
0.33 μM caf
0.5 μM caf
0.66 μM caf
0.83 μM caf
1 μM caf
1 μM caf H2O
b
0 μM
1 μM
0.05 mg/ml PGM
0.17 μM VC5
0.33 μM VC5
0.5 μM VC5
0.66 μM VC5
0.83 μM VC5
1 μM VC5
1 μM VC5 H2O
c
0 μM
1 μM
0.05 mg/ml PGM
0.17 μM VC5-caf
0.33 μM VC5-caf
0.5 μM VC5-caf
0.66 μM VC5-caf
0.83 μM VC5-caf
1 μM VC5-caf
1 μM VC5 H2O
1 μM caf H2O
d
0 μM
1 μM
0.05 mg/ml PGM
0.17 μM VC10
0.33 μM VC10
0.5 μM VC10
0.66 μM VC10
0.83 μM VC10
1 μM VC10
1 μM VC10 H2O
e
0 μM
1 μM
0.05 mg/ml PGM
0.17 μM VC10-caf
0.33 μM VC10-caf
0.5 μM VC10-caf
0.66 μM VC10-caf
0.83 μM VC10-caf
1 μM VC10-caf
1 μM VC10 H2O
1 μM caf H2O
f
1 μM
0 μM
0.05 mg/ml PGM
0.17 μM AC10
0.33 μM AC10
0.5 μM AC10
0.66 μM AC10
0.83 μM AC10
1 μM AC10
1 μM AC10 H2O
g
1 μM
0 μM
0.05 mg/ml PGM
0.17 μM AC10-caf
0.33 μM AC10-caf
0.5 μM AC10-caf
0.66 μM AC10-caf
0.83 μM AC10-caf
1 μM AC10-caf
1 μM AC10 H2O
1 μM caf H2O

Figure 3

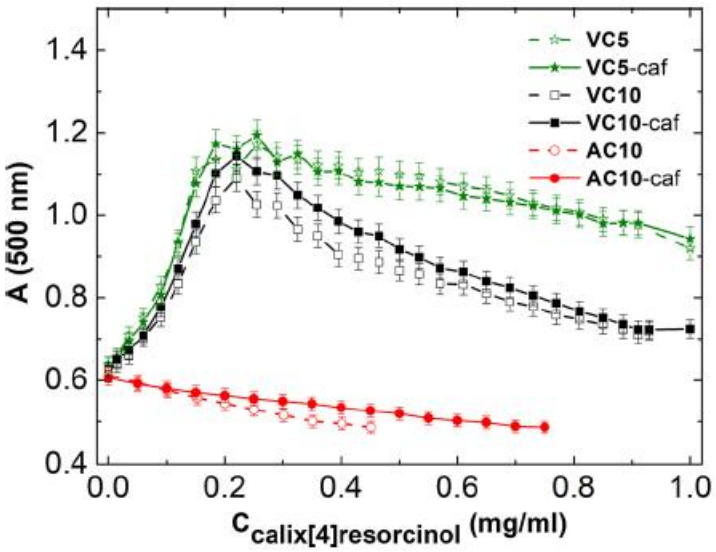

Figure 4

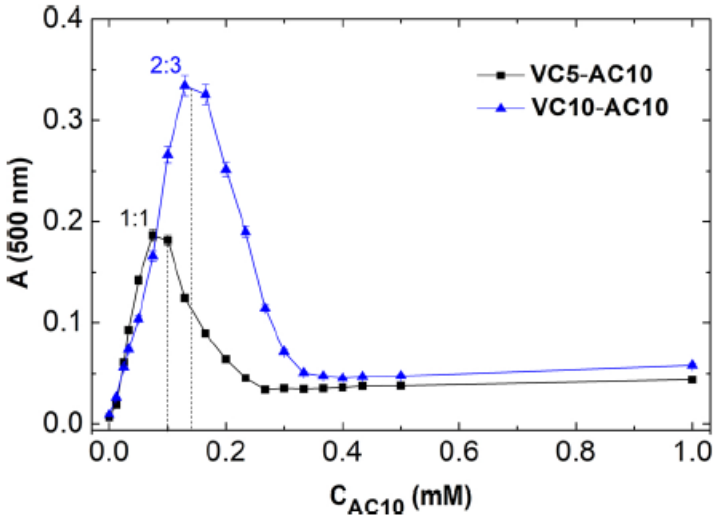

Figure 5

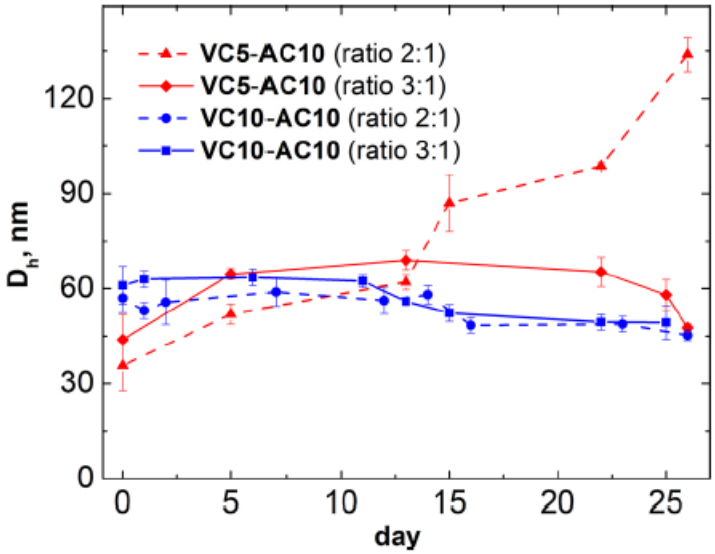

Figure 6